Polyhedron 139 (2018) 215–221

Contents lists available at ScienceDirect

Polyhedron

journal homepage: www.elsevier.com/locate/poly

Seven-coordinate tetraoxolate complexes

Andrew N. Simonson [a,b], Christopher M. Kareis [a,b], Nikolaii S. Ovanesyan [c], David O. Baumann [a,b], Arnold L. Rheingold [d], Atta M. Arif [b], Joel S. Miller [a,b,*]

[a] Material Research Science and Engineering Center, University of Utah, Salt Lake City, UT 84112, USA
[b] Department of Chemistry, University of Utah, Salt Lake City, UT 84112-0850, USA
[c] Institute of Problems of Chemical Physics, Russian Academy of Science, Chernogolovka, Russia
[d] Department of Chemistry, The Department of Chemistry, University of California, San Diego, La Jolla, CA 92093-0358, USA

ARTICLE INFO

Article history:
Received 30 July 2017
Accepted 13 October 2017
Available online 17 October 2017

Keywords:
Antiferromagnetic interaction
Tetraoxolate
Mn complex
μ-Oxo-diiron complex
Mössbauer

ABSTRACT

The reaction of TPypA (tris(2-pyridylmethyl)amine) and $Fe(BF_4)_2$ and sodium nitranilate ($Na_2\mathbf{1_{NO2}}$) or $Mn(O_2CMe)_2$ with chloranilic acid ($H_2\mathbf{1_{Cl}}$) respectively forms $[Fe^{III}(TPyA)\mathbf{1_{NO2}}]_2O$ and $Mn^{II}(TPyA)\mathbf{1_{Cl}}$, respectively. The structures of these 7-coordinate compounds have been determined. The former is a dinuclear Fe^{III} compound possessing equivalent Fe(III) sites, and the latter forms a 1-D zigzag chain based upon the two bridging $\mathbf{1_{NO2}}^{2-}$ ions. The isomer shift and quadrupole splitting of the ^{57}Fe Mössbauer spectra of $[Fe(TPyA)\mathbf{1_{NO2}}]_2O$ are consistent binuclear seven-coordinate high-spin Fe^{III} state. Below 35 K a single quadrupole doublet split onto two doublets of equal intensities and equal isomer shifts as a result of structural non-equivalency of two iron sites within a dimer. The magnetic properties of $[Fe^{III}(TPyA)\mathbf{1_{NO2}}]_2O$ can be fit the a homonuclear $S = 5/2 \pm 5/2$ dinuclear spin model with strong intradimer antiferromagnetic coupling of $J/k_B = -146$ K (-101 cm^{-1}) and $g = 2.00$, and interdimer coupling of $\theta = -5$ K ($H = -2JS_a \cdot S_b$). $Mn^{II}(TPyA)\mathbf{1_{Cl}}$ can be fit the a homonuclear $S = 5/2$ 1-D Fisher chain expression with weak intrachain antiferromagnetic coupling with $J/k_B = -0.33$ K (-0.23 cm^{-1}) and $g = 2.06$.

1. Introduction

Dinuclear metal complexes bridged with chloranilate (CA^{2-}) [1] (**1**: R = Cl, $\mathbf{1_{Cl}}$) and related tetraoxolates [2] having a delocalized π system have been shown to exist in different oxidation states and exhibit unusual magnetic behaviors, as well as reduction leading to oxidation [3,4]. The Co-based $[(TPyA)Co^{II}(CA^{2-})Co^{II}(TPyA)](BF_4)_2$ [TPyA = tris(2-pyridylmethyl)amine] dinuclear complex shows weak antiferromagnetic interactions, while Fe-based $[(TPyA)Fe^{II}(CA^{2-})Fe^{II}(TPyA)](BF_4)_2$ exhibits weak ferromagnetic interactions. In addition, species with $CA^{\cdot 3-}$ present in dinuclear cobalt and iron complexes exhibit much stronger spin coupling than those with CA^{2-}, due to direct spin coupling to the radical. Furthermore, the formation of $CA^{\cdot 3-}$ in $[(TPyA)Co^{III}(CA^{\cdot 3-})Co^{III}(TPyA)](BF_4)_3$ occurred via a redox-induced electron transfer (RIET) reaction [5], in which addition of one equivalent of an oxidant results in the oxidation of two metal centers and reduction of the CA^{2-} bridging ligand [6]. In contrast, the iron(II) dinuclear complex bridged with DBQ^{2-} (DBQ^{2-} = 2,5-di-*tert*-butyl-3,6-dihydroxy-1,4-benzoquinonate), i.e. $[(TPyA)Fe^{II}(DBQ^{2-})Fe^{II}(TPyA)](BF_4)_2$, exhibits spin crossover behavior around room temperature [7]. In general, the electronic structures and magnetic behaviors of these dinuclear complexes are very sensitive to the substituent on the bridging anilate ligand. To further explore this chemistry we investigated the reaction of Mn(II) with H_2CA and Fe(II) with the more electron withdrawing nitranilate, **1**: R = NO_2, $\mathbf{1_{NO2}}$. Herein, we report the synthesis of seven-coordinate compounds of $Mn^{II}(TPyA)\mathbf{1_{Cl}}$ and $[Fe^{III}(TPyA)\mathbf{1_{NO2}}]_2O$ composition, as well as their magnetic behaviors.

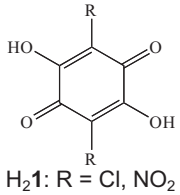

H_2**1**: R = Cl, NO_2

2. Experimental

2.1. General procedures

All chemicals used in the synthesis were of reagent grade and used without further purification. Tris(2-pyridylmethyl)amine

* Corresponding author at: Material Research Science and Engineering Center, University of Utah, Salt Lake City, UT 84112, USA. Fax: +1 801 5818433.
E-mail address: jsmiller@chem.utah.edu (J.S. Miller).

https://doi.org/10.1016/j.poly.2017.10.016
0277-5387/

(TPyA) [8] and sodium nitranilate ($Na_2\mathbf{1}_{\mathbf{NO2}}$, $\mathbf{1}_{\mathbf{NO2}}{}^{2-}$) [9] were prepared according to literature procedures. Iron(II) tetrafluoroborate hexahydrate, $Fe(BF_4)_2{\cdot}6H_2O$, manganese acetate tetrahydrate, $Mn(O_2CMe)_2{\cdot}4H_2O$, triethylamine, and chloranilic acid (H_2CA, CA^{2-}) were used as received. Solvents were used without further purification. Unless stated otherwise all syntheses were performed under aerobic conditions. Infrared spectra were recorded with a Bruker Tensor 37 FT-IR spectrophotometer (±1 cm^{-1}). Magnetic susceptibilities were measured in applied fields of 1 kOe between 2 and 300 K on a Quantum Design MPMS superconducting quantum interference device (SQUID) magnetometer as previously reported [10]. Diamagnetic corrections [586×10^{-6} (Mn^{II}(TPyA)$\mathbf{1}_{\mathbf{Cl}}$), and 604×10^{-6} ([Fe^{III}(TPy$\mathbf{1}_{\mathbf{NO2}}$]$_2$O) emu/mol] were determined by using Pascal's constants.

2.2. Synthesis

2.2.1. Synthesis of [(TPyA)($\mathbf{1}^{2-}_{NO2}$)Fe^{III}(μ-O)Fe^{III}($\mathbf{1}^{2-}_{NO2}$)(TPyA)]

To an MeCN solution (20 mL) of $Fe(BF_4)_2{\cdot}6H_2O$ (177 mg, 0.524 mmol) was added an MeCN solution (20 mL) of TPyA (152 mg, 0.524 mmol). The color turned deep red and the solution was stirred for 10 min at room temperature. $Na_2\mathbf{1}_{\mathbf{NO2}}{\cdot}2.5H_2O$ (141 mg, 0.515 mmol) was then added as a solid to the red solution along with additional MeCN (10 mL) and the mixture was heated to reflux for 4 h. After filtration while hot through Celite, the dark green–brown solution was allowed to stand for 4 days. Dark red crystals formed that were collected by filtration, washed with cold MeCN (5 mL) and dried in air to afford 160 mg (53%) of [(TPyA)($\mathbf{1}^{2-}_{NO2}$)Fe^{III}]$_2$O. Key IR (cm^{-1}; KBr): 1653 m, 1582 s, 1565 s, 1496 m, 1448 m, 1399 m, 1316 m, 910 m, 820 m.

2.2.2. Synthesis of Mn^{II}(TPyA)$\mathbf{1}_{Cl}$·MeOH

A solution of $Mn(O_2CMe)_2{\cdot}4H_2O$ (64.0 mg; 0.262 mmol) dissolved in 15 mL of methanol was added to a solution of TPyA (100 mg, 0.344 mmol) dissolved in 7 mL of methanol in a 100 mL round bottom flask. To the resulting pale-pink solution was added of chloranilic acid (36.0 mg; 0.172 mmol) dissolved in 10 mL of methanol resulting in a dark purple solution and formation of a dark precipitate. To the mixture was added 0.05 mL (0.344 mmol) triethylamine and was then refluxed for 30 min. After filtration while hot, the dark purple solution was allowed to stand for 3 days upon which dark red crystals formed. The crystals were collected and washed with 5 mL of methanol and allowed to dry in air (Yield: 79 mg, 38%). Key IR (cm^{-1}; KBr): 1604 m, 1557 s, 1494 s, 1434 m, 1377 m, 1356 m, 1017 m, 992 m, 865 m, 840 m, 765 m, 578 m.

2.3. X-ray structure determination of (TPyA)($\mathbf{1}^{2-}_{NO2}$)Fe^{III}(μ-O)Fe^{III}($\mathbf{1}^{2-}_{NO2}$)(TPyA) and Mn^{II}(TPyA)$\mathbf{1}_{Cl}$·MeOH

Crystals of Mn^{II}(TPyA)$\mathbf{1}_{\mathbf{Cl}}$ and [Fe(TPyA)$\mathbf{1}_{\mathbf{NO2}}$]$_2$O were mounted on a CryoLoop® with Paratone® oil. A plate $0.25 \times 0.23 \times 0.03$ mm crystal of Mn^{II}(TPyA)$\mathbf{1}_{\mathbf{Cl}}$ was studied on a Nonius KappaCCD diffractometer equipped with Mo Kα radiation (λ = 0.71073 Å). Ten frames of data were collected at 150(1) K with an oscillation range of 1°/frame for 20 s/frame. Indexing and the unit cell refinement was based on all observed reflection from those ten frames, indicated a triclinic P lattice. A total of 9623 reflections (Θ_{max} = 25.99°) were indexed, integrated and corrected for Lorentz, polarization and absorption effects using DENZO-SMN and SCALEPAC [11]. Axial photographs and systematic absences were consistent with the compound having crystallized in the triclinic $P\bar{1}$ space group. The structure was solved by a combination of direct methods and heavy atom using SIR97 [12]. All non-hydrogen atoms were refined with anisotropic displacement coefficients. Hydrogen atoms were assigned isotropic displacement coefficients U(H) = 1.2U(C) or 1.5U(C_{methyl}), and their coordinates were allowed to ride on their respective carbons using SHELXL97 [13]. The weighting scheme employed was $w = 1/[\sigma^2(F_o^2) + (0.0742P)^2 + 2.8425P]$ where $P = (F_o^2 + 2F_c^2)/3$. The refinement converged to $R1$ = 0.0555, $wR2$ = 0.1526, and S = 1.105 for 4254 reflections with $I > 2\sigma(I)$, and $R1$ = 0.0678, $wR2$ = 0.1609, and S = 1.105 for 5100 unique reflections and 337 parameters, where S = Goodness-of-fit on F^2 = [$\Sigma(w(F_o^2 - F_c^2)^2/(n-p)]^{1/2}$, and n is the number of reflections and p is the number of parameters refined. The maximum Δ/σ in the final cycle of the least-squares was zero, and the residual peaks on the final difference-Fourier map ranged from −0.791 to 0.758 e/Å^3. Scattering factors were taken from the International Tables for Crystallography, Volume C [14].

Multi-scan intensity data after being corrected for absorption using the SADABS program [13] for [Fe(TPyA)$\mathbf{1}_{\mathbf{NO2}}$]$_2$O was collected with a Bruker APEX CCD detector, and the data were integrated using the Bruker SAINT software program [13,15]. The structures were solved by direct methods and refined by full-matrix least-squares methods using SHELXL97 [13]. The positions of all non-hydrogen atoms were refined with anisotropic displacement factors. All hydrogen atoms were placed using a riding model, and their positions were constrained relative to their parent atom using the appropriate HFIX command in SHELXL97. The crystallographic data of [Fe^{III}(TPyA)$\mathbf{1}_{NO2}$]$_2$O and Mn^{II}(TPyA)$\mathbf{1}_{Cl}$, are summarized in Table 1. Images of structures generated using CrystalMaker®; CrystalMaker Software Ltd, Oxford, UK.

2.3.1. ^{57}Fe Mössbauer determination of [(TPyA)($\mathbf{1}^{2-}_{NO2}$)Fe^{III}(μ-O)Fe^{III}($\mathbf{1}^{2-}_{NO2}$)(TPyA)]

The ^{57}Fe Mössbauer spectra vs. metallic iron at room temperature were recorded with a constant acceleration spectrometer (Wissel GMBH) using a *ca.* 25 mCi ^{57}Co/Rh source. Low temperature spectra are measured using continuous-flow helium cryostat (CF-506, Oxford Instr. Ltd) operating in the temperature range 4.2 to 305 K. The Mössbauer spectra comprised single quadrupole doublet that was solved by least-squares refinement of Lorentzian shape peaks. Below 35 K the two-doublet split spectra were satisfactorily fitted using two-state relaxation model.

Table 1
Summary of the crystallographic data for Mn^{II}(TPyA)$\mathbf{1}_{Cl}$·MeOH and [Fe^{III}(TPyN)$\mathbf{1}_{NO2}$]$_2$O.

	Mn^{II}(TPyA)$\mathbf{1}_{Cl}$·MeOH	[Fe^{III}(TPyA)$\mathbf{1}_{NO2}$]$_2$O
Formula	$C_{25}H_{22}Cl_2MnN_4O_5$	$C_{48}H_{36}Fe_2N_{12}O_{17}$
M_W	584.31	1164.58
Crystal system	triclinic	orthorhombic
Space group	$P\bar{1}$	$C222_1$
a (Å)	10.1046(4)	12.8103(10)
b (Å)	12.2317(5)	20.7703(10)
c (Å)	12.2994(4)	19.3874(11)
α (°)	80.160(2)	90
β (°)	69.015(3)	90
γ (°)	66.9351(18)	90
V (Å^3)	5265.0(7)	5158.5(6)
Z	2	4
D_{calc} (g cm^{-3})	1.487	1.500
T (K)	150(1)	113(2)
μ MoK$_\alpha$ (mm^{-1})	0.754	0.647
Flack Parameter	-	0.009(6)
R_1[a] ($I > 2\sigma$)	0.0555	0.0314
wR_2[b] ($I > 2\sigma$)	0.1526	0.0810
Largest diff. peak/hole, e$^-$ Å^{-3}	0.76/−0.79	0.79/−0.21
Goodness-of-fit on F^2	1.105	1.030
CCDC#	1560945	1560768

[a] $R_1 = \Sigma||F_o| - |F_c||/\Sigma|F_o|$.
[b] $wR_2 = [\Sigma w(F_o^2 - F_c^2)^2/\Sigma w(F_o^2)^2]^{1/2}$.